Performance prediction of serpentine type compact magnetorheological brake prototype

Cite as: AIP Conference Proceedings **1788**, 030032 (2017); https://doi.org/10.1063/1.4968285
Published Online: 03 January 2017

Ubaidillah, A. Wibowo, D. Adiputra, et al.

Performance Prediction of Serpentine Type Compact Magnetorheological Brake Prototype

Ubaidillah[1,a)], A. Wibowo[1], D. Adiputra[2], D.D.D.P. Tjahjana[1], M.A.A. Rahman[2], and S.A. Mazlan[2]

[1]*Mechanical Engineering Department, Universitas Sebelas Maret, Surakarta, Jawa Tengah, Indonesia 57126*
[2]*Malaysia-Japan International Institute of Technology, Universiti Teknologi Malaysia, Kuala Lumpur, Malaysia 54100*

[a)]Corresponding author: ubaidillah@uns.ac.id

Abstract. A magnetorheological brake (MRB) with serpentine flux type for ankle-foot orthosis (rehabilitation device) was assessed its performance regarding braking torque and dynamic range. This assessment was conducted based on a problem that the MRB did not generate sufficient braking torque for the orthosis device. The braking capability was appraised through analytical approached based on the prototype design. The magnetic circuit of the MRB design was firstly investigated its capability for generating magnetic flux at braking surface area using finite element method magnetic (FEMM) software. Governing equation was derived to determine the braking performance i.e. braking torque and dynamic range as a function of applied current. The main factors influencing the braking performance were magneto-induced shear stress, the clearance between rotor and stator, and braking surface area. Especially for shear stress, this factor was totally influenced by the magnetic flux generated within the braking area. These all factors were contained within the governing equation. Furthermore, the braking performances were determined by solving the governing equation according to the design parameters. As a result, the governing equation can be used for improving the MRB design to get a better braking performances.

INTRODUCTION

Magnetorheological (MR) fluids have been widely used for smart damping devices such as MR damper, MR brake, MR engine mounting and MR haptic device[1]. The use of MR fluids in the braking system has been revolutionary changing mechanical brake to the brake-by-wire system in which it is less employing mechanical parts [2]. The working principle of MR brake is a dissipation of energy resulted from rotor into another form of energy by manipulating the shear stress of MR fluids within the gap between rotor and stator. The change of shear stress is usually accommodated by treating MR fluids with magnetic fields. Meanwhile, the magnetic fields are provided from electromagnetic parts embedded within the MR brake. Some magnetic fields depend on the electric current generated by the electromagnet. It is, therefore, the alteration of shear stress can be achieved in the ranges of milliseconds (less than 10 milliseconds) [3].

Penetration of MR brake in some application such as automotive braking system, rotary damper, joystick, and medical rehabilitation devices has challenged researchers to develop various types and design. Numerous types of MR brake have been proposed and assessed such as disc type, drum type, T-shaped MRBs, multiple disks, and multiple coils [4]. These types were proposed based on typical application. Although, the MR brake has been tried to be applied in the tremendous application, one of the main drawback is less producing braking torque compared to the mechanical brake. So far, the application of high torque MR brake was conducted by Sohn et al. [5] which utilizing MR brake in middle size motorcycle. The maximum torque achieved by the optimized design was more than 100 Nm. This excellent result was achieved after optimization on the MR brake design. Based on the drawback, existing research on MR brake mostly penetrated low brake application such as haptic and medical rehabilitation devices. Utilization of MR brake for rehabilitation medical device has been previously conducted. Avraam et al. [4,6] proposed solicitation of MR brake

International Conference on Engineering, Science and Nanotechnology 2016 (ICESNANO 2016)
AIP Conf. Proc. 1788, 030032-1–030032-8; doi: 10.1063/1.4968285
Published by AIP Publishing. 978-0-7354-1452-5/$30.00

for wrist rehabilitation device. T-shaped MR brake was adopted for this application. Another application for rehabilitation medical device was MR brake for controllable ankle-foot orthoses by Kikuchi et al. [7,8]. This controllable ankle foot orthosis was utilized for ankle rehabilitation. A compact multiple disc type MR brake having a size of 52 mm total diameter and 32 mm thick which available torque was about 4 Nm. This design was indeed achieving high torque since it used 18 layers MR fluids with micron sized gap. However, the fabrication of multiple disks in a compact size would need advanced machining process due to very high tolerances.

All of MR brake designs have mostly the same strategy for reaching optimum braking torque or dynamic ranges that are improving effective braking area or friction area. As proposed by Senkal and Gurocak [9], a compact serpentine type MR brake is proposed in this study to achieve maximum braking area in a limited size of MR brake. For information, this MR brake would be integrated into ankle-foot orthoses for foot drop prevention. This kind of disorder usually happens in the post-stroke patient. Since the application is for foot swinging, the overall mass of ankle-foot orthoses should be as light as possible. This paper delivers the first step development of MR brake that is design and braking performance prediction of the device. The discussion covers design, working principle, mathematical model, magnetic circuit analysis, finite element method magnetic, and braking torque performance prediction.

METHODOLOGY

Design of MR Brake

As stated before, the compact MR brake with serpentine flux type was dedicated for ankle-foot orthoses. Therefore, the size and mass were limited to a constraint that the design has a maximum size of 45 mm and thickness of 30 mm. The 3D model of MR brake including its cross-sectional view is depicted in Fig. 1. A rotor and a stator construct the compact MR brake. The rotor consists 6 parts namely: rotor shaft (1 pc, bronze), rotor steel (3 pcs, AISI 1020), and spacer (2 pcs, bronze). Meanwhile, the stator is constructed of main wall (AISI 1020), o-ring (rubber), rubber seal (rubber), a spacer (bronze), bobbin (bronze), and wire coil (copper). The structure of rotor steel, stator steel, and spacers as shown in Fig. 1 is objected to making all surface in the rotor can be magnetized. Hence, the shear stress occurs optimally. The flow of magnetic flux can be seen in section finite element method magnetic. Based on the existing structure, we predicted that the spacer could bend the flux flow. Hence, the flow pattern is similar to meandering shape or for the appropriate term, serpentine pattern. In this device planning, MRF-132DG, Lord Corp. was utilized as a braking medium. The technical specification and relationship between shear yield stress and flux density are shown in Table 1 and Fig. 2, respectively.

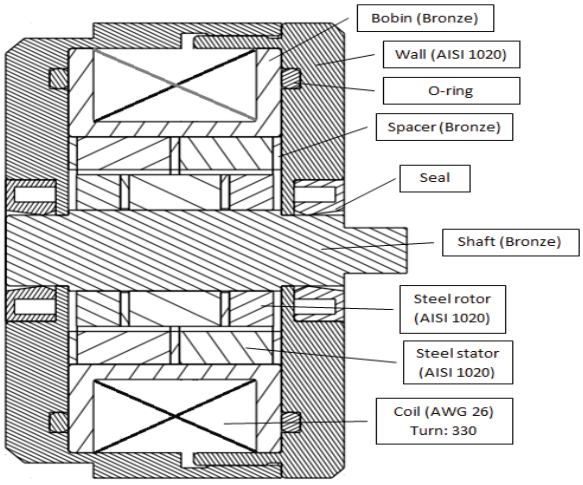

FIGURE 1. The design of MR brake.

TABLE 1. Specification of MR fluids MRF-132DG

Property	Value/limits
Based fluid	Hydrocarbon
Work temperature	-40 to 130°C
Density range	2.98 to 3.18g/cm^3
Solid percentage weight	80.98%
Specific heat @ 25°C	0.79 $J/g°C$

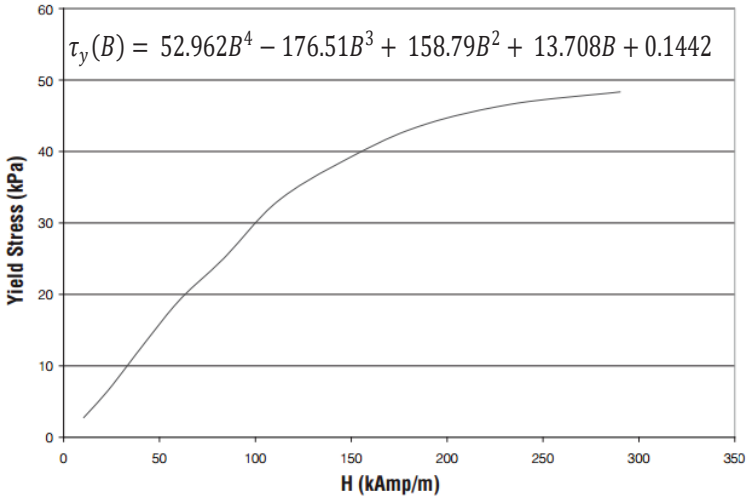

FIGURE 2. The relationship between shear yields stress and magnetic fields.

Braking Torque Model

The design of compact MR brake was firstly predicted its capability for generating the braking torque. As can be seen in Fig. 3, the braking torque results from the summation between viscous (off state) and magneto-induced torques (on state). Based on Figure 3, the both annular and radial area contribute to the braking torque. Each torque value can be calculated based on equations stated in Table 2. On state torque depends on the shear yield stress values which are influenced by a number of magnetic fields. The shear yields stress τ_y is obtained from the MR fluids characteristics as depicted in Figure 2 and the polynomial relationship is governed based on the shear yield stress data. The polynomial equation representing shear yield stress characteristic can be viewed in Fig. 2.

TABLE 2. List of equation used for braking torque calculation

Torque value, radial (off state)	$\boldsymbol{T_{\eta\, radial} = \frac{\pi\eta\dot{\theta}}{g}\left[R_r^4 - R_i^4\right]}$
Torque value, annular (off state)	$T_{\eta\, annular} = 2\pi h\eta\frac{\dot{\theta}}{g}R_r^3$
Total torque (off state)	$T_\eta = \frac{\pi\eta\dot{\theta}}{g}[R_r^4 - R_i^4] + 2\pi h\eta\frac{\dot{\theta}}{g}R_r^3$
Torque value, radial (on state)	$T_{\tau\, radial} = \frac{2}{3}\pi\tau_y(R_r^3 - R_i^3)$
Torque value, annular (on state)	$T_{\tau\, annular} = 2\pi h\tau_y R_r^2$
Total torque (on state)	$T_\tau = T_{off-state} + T_{on-state}$

The value of shear yield stress is proportional to the generated magnetic flux flow through the MR fluids. The magnetic flux enhanced when the current applied to the coil increases. Therefore, there are two strategies capable of

increasing magnetic flux those are either increasing the electric current on the coil or choosing thinner copper wire size to get a larger amount of coil winding. Increasing current is not a good choice for limited space of coil winding since it will generate heat. Thus, the appropriate alternative for limited space of MR brake is choosing thin copper wire diameter. In this study, the diameter of the copper wire is 0.45 mm (AWG26). The thinner size can be selected. However, it will limit the maximum chassis current transmitted through the copper wire. Whereas, this design required maximum current applied about 2 A.

The base dimensions used for braking torque performance calculation are detailed in Table 3. The radial and annular gap were initially set to 0.65 and 0.5 mm. The calculation of MR brake performance will also cover the changes of both annular and radial gaps size. This step is necessary for knowing the effect of gap turning to the MR brake performance.

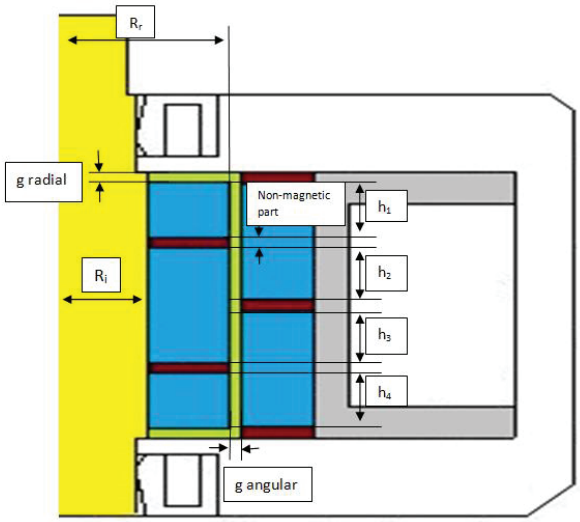

FIGURE 3. The configuration of rotor and stator.

TABLE 3. MR brake dimension.

No	Symbol	Description	Value
1	π	Phi/constant	22/7
2	η	Viscosity of base fluid (Pa.s)	0,112
3	$\dot{\theta}$	Rotational velocity (rad/s)	1,046
4	g	Radial gap (mm)	0,45
		Angular gap (mm)	0,3
5	R_r	Outer rotor radius (mm)	7,7
6	R_i	Inner rotor radius (mm)	4,0
7	h	Angular channel length 1 (mm)	3,7
		Angular channel length 2 (mm)	3,3
		Angular channel length 3 (mm)	3,3
		Angular channel length 4 (mm)	3,7
		Angular non-magnetic area/spacer (mm)	0,7
8	τ_y	Shear yield stress of the MR fluids (MPa)	

Magnetic Circuit

It is important to establish the magnetic circuit of the designed MR brake. The magnetic circuit will confirm the flux flow along the circuit and it can also be used for initial prediction of magnetic field density generated by the electromagnet. Besides, material selection can be firstly determined by considering the magnetic circuit. Kirchhoff Laws is useful to derive the magnetic circuit in one loop system. Based on the design configuration, there are 13

reluctances construct the magnetic circuit such as $\Re_{coil1}$ (1 segment), $\Re_{wall}$ (1 segment), $\Re_{MR}$ fluids (6 segments), $\Re_{rotor\ steel}$ (3 segments), $\Re_{stator\ steel}$ (2 segments). Equation (Eq. 1) can be utilized for determining the reluctance of each section as follows,

$$\Re = \frac{L}{\mu A} \tag{1}$$

Where, L is the effective length that passed by the magnetic flux in each section, μ is the magnetic permeability, and A is the effective area of the magnetic flux. Moreover, Equation (Eq. 2) shows the total magnetomotive force which is the summation of the magnetomotive force generated by all of the parts in one loop. The magnetomotive force is directly proportional to the magnetic flux and reluctance as expressed in below,

$$\Phi_1 - \Re_{coil1} - \Re_{wall} - \Re_{mrfluid} - \Re_{rotorsteel} - \Re_{mrfluid} - \Re_{statorsteel} - \Re_{mrfluid} - \Re_{rotorsteel} - \Re_{mrfluid} - \Re_{statorsteel} - \Re_{mrfluid} - \Re_{rotorsteel} - \Re_{mrfluid} = 0 \tag{2}$$

The magnetic flux ϕ_1 depends on the number of coil turns and electric current pass through the coils. Therefore, Eq.2 can be rewritten as the following Eq.3,

$$N_1 I_1 - \Re_{coil1} - \Re_{wall} - \Re_{mrfluid} - \Re_{rotorsteel} - \Re_{mrfluid} - \Re_{statorsteel} - \Re_{mrfluid} - \Re_{rotorsteel} - \Re_{mrfluid} - \Re_{statorsteel} - \Re_{mrfluid} - \Re_{rotorsteel} - \Re_{mrfluid} = 0 \tag{3}$$

where *N*, and *I* are a number of wire turns in each coil, and electric current passing through the coils, respectively.

RESULTS AND DISCUSSION

Finite Element Method Magnetic (FEMM)

Magnetic flux pattern within the MR brake was studied using free license software namely FEMM (Finite Element Methods Magnetics) Version 4.2. During the first step, half of longitudinal cross section of the MR brake was drawn in axisymmetric mode. It was followed by material assignment following the software library. In case, the software does not provide non-standard material, such as MR fluids, the magnetic permeability can be inputted to the software manually. Meshing process was followed after material assignment. The model could then be run by applying an electric current, particularly. The current applied during simulation was particularly 0.1 until 2 A by interval 0.1 Amperes. Figure 4 portrays the distribution of magnetic fields at driven current 0.1, 1 and 2 Amperes. From the figure, it can be seen that the magnetic field intensity increases at the increment of electric current marked by the red color at the effective braking area.

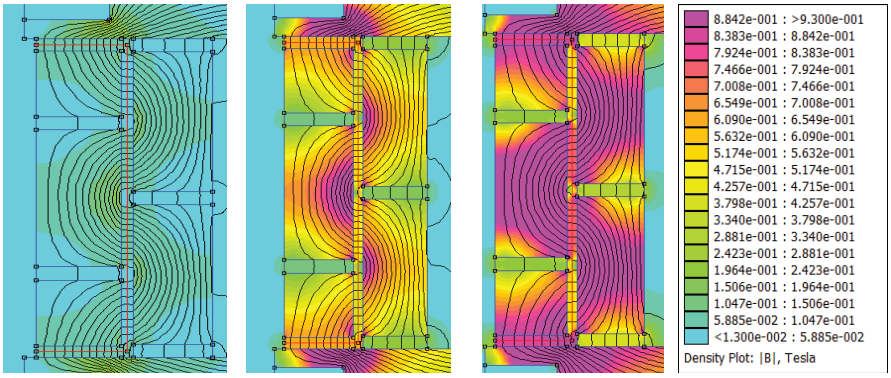

FIGURE 4. Magnetic fields distribution

Figure 5 depicts flux density values at MR fluids area. It can be seen that the flux density varies from 0.3 – 0.87 T at the radial area as well as 0.2 – 0.54 T and 0.25 – 0.78 T at the annular area. The figure only shows flux density value for applied current of 0.4, 0.8, 1.2, 1.6, and 2.0 A. The difference of flux enhancement at the small current applied, especially below 1 A, is quite extensive compared to the higher current. This fact is because the achieved flux value closes the magnetization saturation of the magnetic materials. Therefore, the application of current upper 2 A will not provide significant improvement of the flux. Instead, application of high current to AWG-26 in practical will burn the copper wire (coil) due to the excessive heat generation. From the result, it can be concluded that the concentration of magnetic fields at radial area contributes higher magneto-induced shear stress compared to the annular area. It can also be inferred that for further design improvement, the radial area can be adjusted its field to increase the active surface.

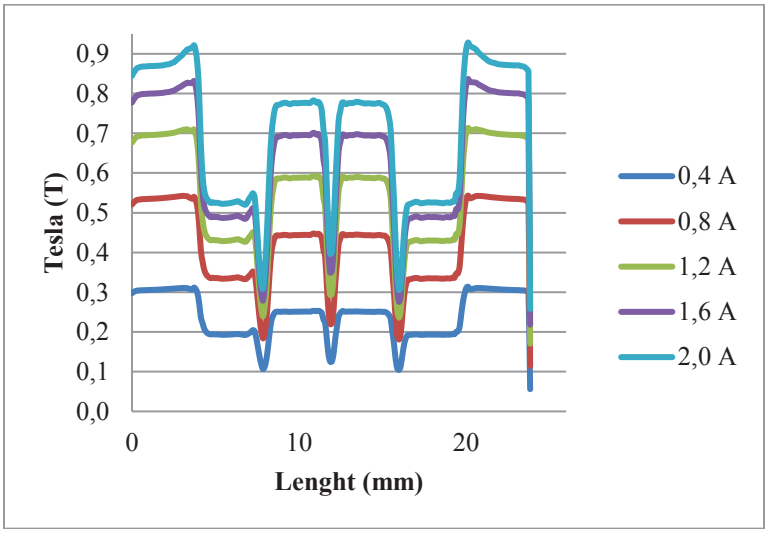

FIGURE 5. Flux density value in MR fluids gap

Performance Prediction

Prediction of achievable torque by the MR brake is portrayed in Figures 6 (a) and (b). The process to obtain torque values were began from magnetic flux data collection resulted by FEMM simulation. The flux values were then operated in shear yields stress equation from the curve fitting. Here, the on state braking torque is dominantly influenced by the amount of shear stress. Meanwhile, the off state braking torque is subjective to the rotor angular speed and MR fluids viscosity.

From Figure 6(a), it can be seen that the torque enhances significantly by the increment of current. The trend of torque increase is not linear since the value depends on the magnetic fields alteration. The maximum torque achieved by the MR brake with radial and annular gaps of 0.65 and 0.5 mm is 0.26 Nm. The dynamic range or magnetorheological effect that is percentage increment between off and on states is calculated about 2500%. This value was the ratio between on and off state torque difference to off state torque which was 0.01 Nm.

The predicted torque value seems quite small and needs to be improved. In this research, the braking torque will be evaluated its alteration by modifying the effect of radial and annular gaps. Here, the radial gap was reduced and increased its size. For radial gap, it was previously 0.65 mm, and further variation would be from 0.45 to 0.85 mm. Meanwhile, the annular gap varies from 0.3 to 0.6 mm from initially 0.5 mm. It was consequently changing the radial size of rotor and stator. Nevertheless, the size of the coil winding and applied current were the same. Predicting the braking torque for the new gap configuration must be carried out from the beginning that is FEMM simulation and so on. Figure 6(b) exhibit the braking torques which can be achieved by the MR brake. It can be seen that the smallest gap provides the highest achievable torque. It increases about 20% from the initial configuration. Moreover, when the gaps increase until the largest gaps, the braking torque reduces until 20%. From the calculated torques, the annular and radial gaps play an important role beside other parameters such as rotor radius and length.

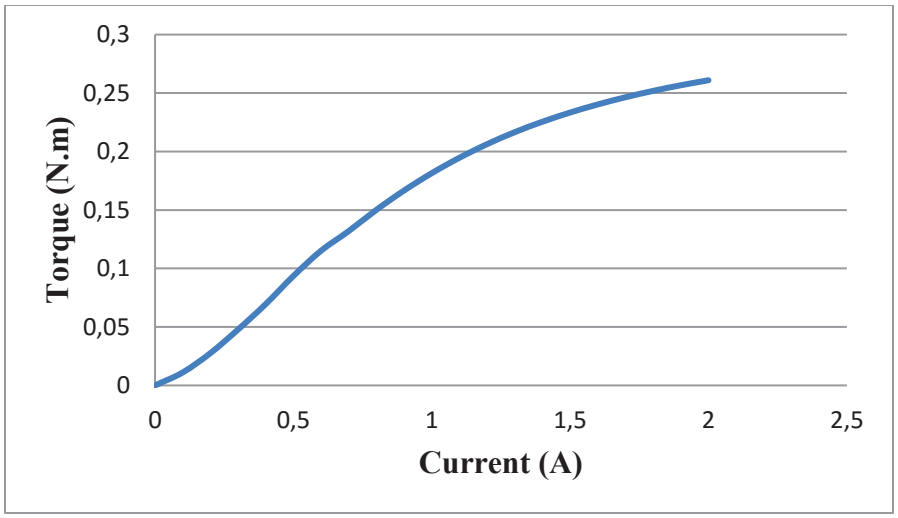

(a)

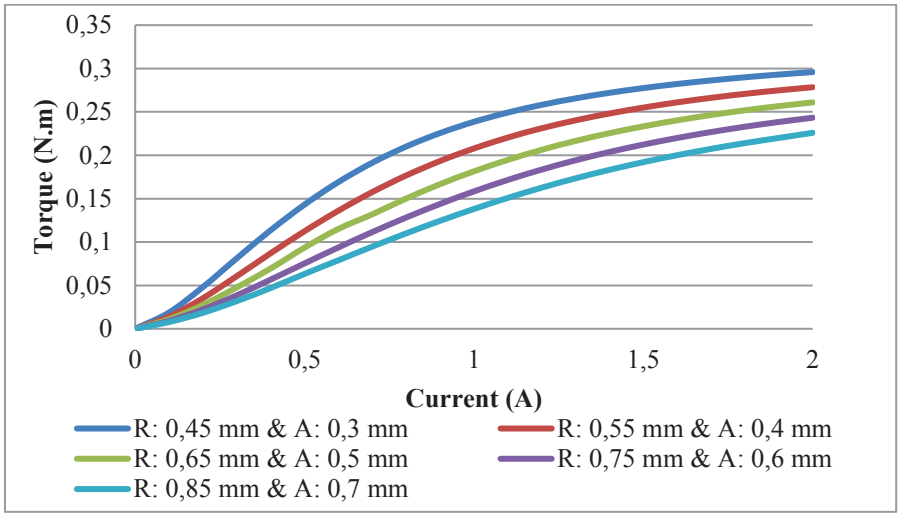

(b)

FIGURE 6. Predicted torque: (a) value at a radial gap of 0.65 mm and an annular gap of 0.5 mm, and (b) varied radial and annular gaps.

CONCLUSION

Performance assessment of compact MR brake featuring serpentine flux has been carefully conducted. Based on the FEMM simulation the configuration of rotor steels, stator steels, and spacer successfully turned the magnetic flux flows. It is, therefore, the effective area could be increased by following the serpentine configuration. Magneto-induced torque achieves about 0.26 Nm for MR brake with radial and annular gaps of 0.65 and 0.5 mm, respectively. The variation of gaps could significantly influence the value of braking torque. The dimension of MR brake can further be improved employing the governed mathematical model.

ACKNOWLEDGEMENTS

We would like to thank the Universitas Sebelas Maret for total financial support for this research. We also thank to Vehicle System Engineering i-Kohza, Malaysia-Japan International Institute of Technology, Universiti Teknologi Malaysia.

REFERENCES

1. Ubaidillah, F. Imaduddin, M. Nizam, and S.A. Mazlan, Int. J. Electr. Eng. Informatics. **7**, 308–322 (2015).
2. F. Imaduddin, S. Amri Mazlan, M. Azizi Abdul Rahman, H. Zamzuri, Ubaidillah and B. Ichwan, Smart Mater. Struct. **23**, 65017 (2014).
3. Ubaidillah, K. Hudha and F.A.A. Kadir, Int. J. Model. Identif. Control. **13**, 9 (2011).
4. M. Avraam, M. Horodinca, I. Romanescu and A. Preumont, J. Intell. Mater. Syst. Struct. **21**, 1543–1557 (2010).
5. J.W. Sohn, J. Jeon, Q.H. Nguyen and S.-B. Choi, Smart Mater. Struct. **24**, 85009 (2015).
6. M.T. Avraam, "MR-fluid brake design and its application to a portable muscular rehabilitation device," PhD Thesis, Universit´e Libre de Bruxelles, 2009.
7. T. Kikuchi, K. Kobayashi, and A. Inoue, J. Intell. Mater. Syst. Struct. **22**, 1677–1683 (2011).
8. T. Kikuchi, S. Tanida, K. Otsuki, T. Yasuda, J. Furusho," Development of third-generation intelligently controllable ankle-foot orthosis with compact MR fluid brake," in *Proc. - IEEE Int. Conf. Robot. Autom.* (2010), pp. 2209–2214.
9. D. Senkal, and H. Gurocak, Mechatronics. **20**, 377–383 (2010).